Hindawi
International Journal of Polymer Science
Volume 2017, Article ID 2581767, 10 pages
https://doi.org/10.1155/2017/2581767

Research Article

Optimizing Delivery Characteristics of Curcumin as a Model Drug via Tailoring Mean Diameter Ranges of Cellulose Beads

Lee Ken Voon, Suh Cem Pang, and Suk Fun Chin

Faculty of Resource Science and Technology, Universiti Malaysia Sarawak, 94300 Kota Samarahan, Sarawak, Malaysia

Correspondence should be addressed to Suh Cem Pang; suhcem@gmail.com

Received 29 May 2017; Accepted 16 August 2017; Published 26 September 2017

Academic Editor: Arthur J. Ragauskas

Spherical cellulose beads with tailored mean diameter between micrometer (20–80 μm) and nanometer (40–200 nm) ranges were fabricated from regenerated cellulose of paper wastes via water-in-oil (W/O) microemulsion and nanoprecipitation processes, respectively. The mean diameter ranges of cellulose beads were precisely controlled via modulating fabrication parameters such as stirring speed, surfactant concentration, cellulose concentration, and reaction temperature. By tailoring their mean diameter ranges and using curcumin as a model drug, cellulose beads with enhanced loading capacities and optimized release kinetic profiles of curcumin were fabricated.

1. Introduction

Being the most abundant natural biopolymer, nontoxic, biodegradable, biocompatible, and low cost, cellulose is commonly being used as the main feedstock of manufacturing industries [1]. Cellulose has been isolated from various natural biomass resources such as printed paper wastes, wood fibres, cotton, wheat straw, coconut husk fibres, sugarcane bagasse, sesame husk, hemp fibre, and banana rachis [2–4]. However, native cellulose has limited applications due to its innate properties including poor solubility in common solvents, tendency to agglomerate, and high solution viscosity [5]. Native cellulose has been modified through physical, chemical, or biological processes for various applications. In recent decades, there are growing interests on value-added utilization of cellulose by fabricating cellulose beads of various mean sizes for potential biomedical and industrial applications such as drug delivery carriers [6–8], plastic fillers [9, 10], and biodegradable adsorbents [11, 12].

Various approaches, such as emulsion solvent evaporation [13], emulsion precipitation [14], and W/O microemulsion [15], are commonly being used for the synthesis of cellulose beads. However, classical emulsion techniques use large amount toxic solvents and strong acid such as hydrochloric acid which cause environmental issues. Besides, the raw materials used for preparing cellulose beads are cellulose derivatives instead of native cellulose such as methylcellulose, ethylcellulose, hydroxycellulose, which in turn lead to higher production cost [16, 17]. Henceforth, it is essential to study the plausibility of fabricating cellulose beads with controllable mean diameters directly from native cellulose using both the W/O microemulsion system and nanoprecipitation techniques.

Microemulsion approach offers thermodynamic stability, solubilizing capability, optical transparency, and isotropicity for synthesizing particles with controlled properties such as size, geometry, morphology, homogeneity, and specific surface area [18]. Among various microemulsion systems, the water-in-oil (W/O) microemulsion system with a low water ratio is more favourable due to its ability to synthesize smaller, well-dispersed, and uniform micrometer-sized particles with the help of an appropriate surfactant to stabilize the microdroplets [19, 20]. Due to the nature of the microelmusion system, nonionic and nontoxic surfactants such as Span 80 or Tween 80 are the preferred choices [21, 22]. The W/O microemulsion has been extensively used in various fields such as biomaterials synthesis and chemical engineering, with the surfactant monolayer providing stabilization by prohibiting direct contacts between water and oil, as well as by reducing the interfacial tension between the two immiscible

phases. Effective dispersion of the aqueous phase in the oil phase leads to the formation of uniform microemulsion droplets which, in turn, help to maintain the shape and size of particles formed [20, 23]. On the other hand, the nanoprecipitation (or solvent displacement) process could be used for the fabrication of cellulose particles of desirable particle size distributions via manipulating the synthesis parameters [24]. Due to its simplicity and reproducibility, the nanoprecipitation process is a favourable approach for the fabrication of nanosized cellulose beads [22, 25].

Herein, we reported the use of paper wastes as the source of native cellulose for fabricating cellulose beads with controllable mean diameter ranges using both W/O microemulsion and nanoprecipitation techniques. Various fabrication parameters such as stirring speed, surfactant concentration, cellulose concentration, and temperature were found to affect the mean diameter of cellulose beads. The cellulose beads were characterized by scanning electron microscopy (SEM), transmission electron microscope (TEM), and BET surface area analyser. The effects of mean diameter of cellulose beads on their drug delivery characteristics were investigated using curcumin as a model drug. By tailoring their mean sizes between the micrometer and nanometer ranges, cellulose beads with enhanced loading capacities and optimized release kinetic profiles of curcumin were fabricated.

2. Experimental

2.1. Materials. Paper wastes were collected from the campus of Faculty of Resource and Science Technology, Universiti Malaysia Sarawak. Sodium dihydrogen phosphate (NaH_2PO_4), alpha-cellulose, and disodium hydrogen phosphate (Na_2HPO_4) were purchased from Sigma Aldrich. Hydrochloric acid (HCl), sodium hydroxide (NaOH), curcumin, urea, thiourea, sorbitan oleate (Span 80), paraffin oil, absolute ethanol, and sodium dodecyl sulfate (SDS) were purchased from Merck. All chemicals were used without further purification. Phosphate buffer saline solution (PBS) was prepared from 1.0 M sodium dihydrogen phosphate (NaH_2PO_4) and 1.0 M disodium hydrogen phosphate (Na_2HPO_4) solutions. Ultrapure water (~18.2 MΩ·cm, 25°C) was obtained from the Water Purifying System (ELGA, Model Ultra Genetic).

2.2. Extraction of Cellulose Fibres. Cellulose fibres were extracted from paper waste samples based on a reported method [26]. Around 100 g of paper waste sample was ground into powder form and dispersed in water by stirring continuously at 2000 rpm for 2 h. The slurry was treated with NaOH solution (12.0 wt%) for 24 h and subsequently with HCl solution (3.0 wt%) at 80°C for 2 h to remove hemicelluloses, lignin, and residual ink. Purified cellulose fibres were washed with ultrapure water and dried in an oven at 60–100°C for 24 h until their water contents were less than 0.5%. The purity of cellulose sample was confirmed by comparing the FTIR spectrum of cellulose sample with that of commercial alpha-cellulose.

2.3. Dissolution of Cellulose Fibres. Cellulose fibres were dissolved by using an aqueous-based solvent system of NaOH/thiourea/urea (NTU) with composition ratio of 8/6.5/8 (% w/v) as described elsewhere [27]. A weighed amount of the cellulose fibres was dispersed and sonicated for 30 min in 100 mL of NTU solvent. The resulting dispersion was then cooled to −20°C in a freezer for 24 hours to form a solid frozen mass and subsequently thawed at room temperature to obtain a clear cellulose solution.

2.4. Fabrication of Micron-Sized Cellulose Beads (μCBs). μCBs were prepared from the cellulose solution using the water-in-oil (W/O) microemulsion method with Span 80 as the surfactant and acetic acid as the precipitating agent. Typically, 0.6 g of Span 80 was dissolved in 20 mL paraffin oil at room temperature and the resulting mixture was stirred for 30 min to obtain a homogenized oil phase. Subsequently, 3.5 mL of cellulose solution was added dropwise into the oil phase with continuous stirring at 1000 rpm for 1 h to form a microemulsion. μCBs were then precipitated by adding 10% acetic acid under vigorous stirring. Cellulose beads were obtained by separating the resulting mixture in a separating funnel and washed once with deionized water and then twice with absolute ethanol to remove residual NTU solvent, paraffin oil, and Span 80. Synthesis parameters such as the stirring speed (250–1250 rpm), quantity of surfactant (0.5–6.0% w/v), cellulose concentration (1.0–5.0% w/v), and reaction temperature (30–100°C) were modulated to control the mean diameter of μCBs formed. Finally, μCBs were either stored in ethanol (20% v/v) at 0–5°C or dried using the critical point dryer (Bal-Tec CPD 030).

2.5. Fabrication of Nanosized Cellulose Beads (nCBs). 1 mL of cellulose solution of various concentrations (0.1–1.0% w/v) was added dropwise to a fixed quantity of absolute ethanol (6 mL) while undergoing ultrasonication. Cloudy precipitation was observed instantaneously, indicating the formation of nanosized cellulose beads. The resulting suspension was centrifuged and the precipitate was rinsed 5 times with absolute ethanol to remove residual NaOH, urea, and thiourea to obtain nCBs.

2.6. Characterization of Cellulose Beads. SEM and TEM micrographs of cellulose beads were obtained using a Scanning Electron Microscope (SEM) (JEOL-SM 6390 LA) and Transmission Electron Microscope (TEM) (JEOL Model 1230), respectively. For SEM, samples were deposited on aluminium stubs, dried in an oven at 60°C, and coated with a layer of platinum using an Auto Fine Coater (JEOL/JFC-1600). The size distribution of cellulose beads was determined with a laser scattering particle size analyser (CILAS 1090, 0.04–500 μm). CBs were dried using the critical point dryer (Bal-Tec CPD 030) and their specific surface area (S_{BET}) of cellulose beads was determined using the BET surface area analyser (Quantachrome Autosorb iQ-AG) based on nitrogen gas sorption at 77 K.

2.7. Loading of Curcumin. About 200 mg of cellulose beads was dispersed in 20 mL of ethanolic curcumin solution at a concentration of 6 mg/L. The resulting suspension was continuously stirred at 250 rpm in darkness at room temperature for 24 h. Subsequently, the cellulose beads were separated from the dispersing medium by centrifugation at 6,000 rpm. The concentration of curcumin remaining in the supernatant was quantified spectrophotometrically using a UV/Vis spectrophotometer (Jasco V-630) at the wavelength of 429 nm [28]. The amount of curcumin loaded onto cellulose beads was calculated based on the concentration of curcumin remaining in the supernatant with reference to the calibration curve of standard ethanolic curcumin solutions. The loading capacity (LC) and loading efficiency (LE) of curcumin were calculated based on (1) and (2), respectively. All experiments were conducted in triplicate.

$$\text{LC (mg/g)} = \frac{\text{Mass of curcumin loaded onto cellulose beads}}{\text{Mass of cellulose beads}}, \quad (1)$$

$$\text{LE (\%)} = \frac{\text{Mass of curcumin loaded onto cellulose beads}}{\text{Mass of curcumin in solution}} \times 100\%. \quad (2)$$

2.8. Release Kinetics of Curcumin. The in vitro release kinetics of curcumin from cellulose beads was carried out in phosphate buffer solution (PBS, pH = 1.2) containing 8 g/L of sodium dodecyl sulfate (SDS) [29]. 50 mg cellulose beads of different mean diameters were added to 50 mL of PBS, and the desired medium pH values were adjusted by adding dilute hydrochloric acid (1.0 wt%). The suspension was stirred slowly with a magnetic stirrer at 37 ± 0.5°C. 3 mL of PBS for 10 h with cellulose beads being taken out and the same volume was replaced with fresh PBS to maintain a constant volume. The amount of curcumin released was determined from the corresponding absorbance values measured at the wavelength of 429 nm against a calibration curve of standard curcumin solutions in PBS with SDS. All experiments were performed in triplicate. The percentage release of curcumin (CR) from cellulose beads was calculated based on

$$\text{CR (\%)} = \frac{\text{Mass of curcumin released}}{\text{Mass of circumin in CBs}} \times 100\%. \quad (3)$$

The release kinetics of curcumin from cellulose beads were further analysed by fitting experimental data to various kinetics models [30, 31]. For the zero-order kinetics, the cumulative percentage of curcumin versus time (in hour) was plotted based on

$$\text{Zero Order: } Q_t = k_o \times t, \quad (4)$$

where Q_t is the cumulative percentage of curcumin released at time t and k_o is the rate constant.

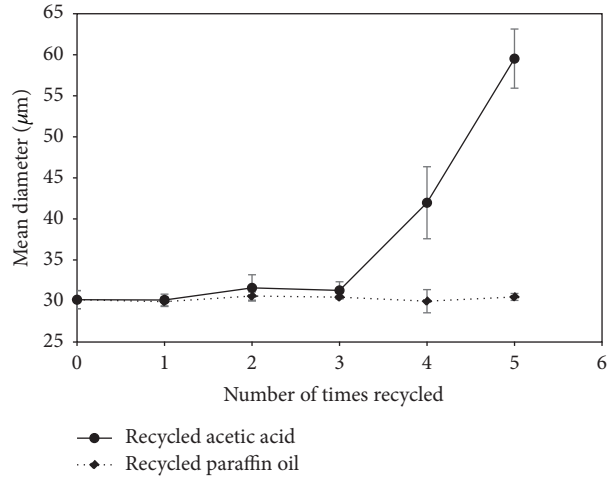

Figure 1: Effect of recycled paraffin oil and acetic acid on the mean diameter of μCBs (3% w/v cellulose solution; 3% w/v Span 80; stirring speed 1000 rpm; 30°C).

Besides, curcumin release kinetics data were being fitted to selected empirical kinetic models including the Higuchi and Korsmeyer-Peppas models as shown by

$$\text{Higuchi: } Q_t = k_{\text{H}} \times t^{1/2}, \qquad \text{Korsmeyer-Peppas: } \frac{M_t}{M_\infty} = k_{\text{KP}} \times t^n, \quad (5)$$

where Q_t is the cumulative percentage of curcumin released at time t; M_t/M_∞ is the fraction of curcumin released at time t; k_{H} and k_{KP} are respective rate constants; and n is the release exponent which is characteristic of different release mechanisms.

3. Results and Discussion

3.1. Fabrication of Micron-Sized Cellulose Beads (μCBs). μCBs fabricated using the water-in-oil microemulsion approach were considerably greener as compared to the conventional method which involved the use of hydrochloric acid as the reaction medium and methanol as the nonsolvent to precipitate micron-sized cellulose beads [32–35]. Besides, both acetic acid and paraffin oil used in the water-in-oil microemulsion approach could be recovered and reused for up to 3 cycles and 5 cycles, respectively, without affecting the mean diameter of μCBs formed (Figure 1). Using the recycled acetic acid for 4th and 5th cycles has led to substantially increased mean diameter of μCBs. This could be attributed to partially neutralized acetic acid with residual NaOH to form acetate salt. Increasing concentrations of acetate, thiourea, and urea dissolved in acetic acid with number of cycles could have rendered it less effective as a precipitating agent. Besides, increased ionic strength of aqueous solution would lead to less stable microemulsion droplets and increased agglomeration of cellulose to form beads of larger mean diameters.

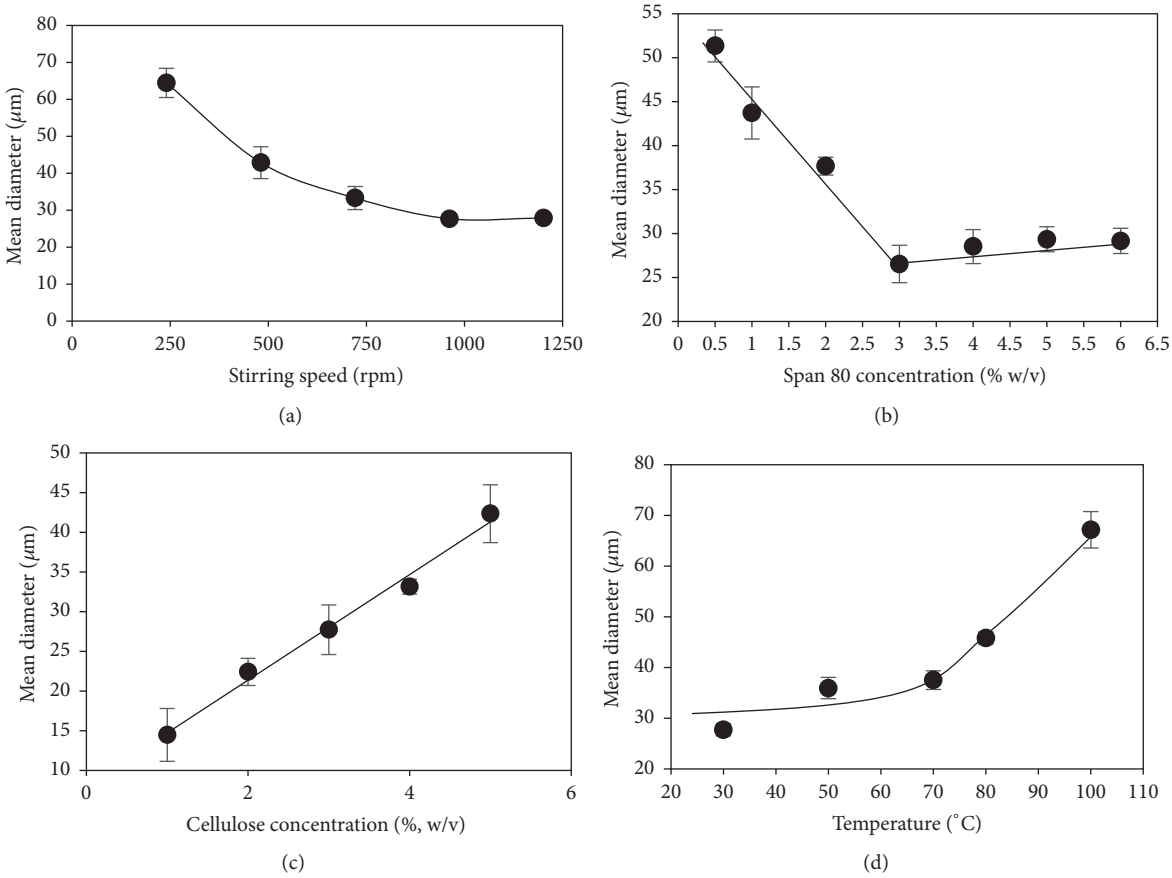

Figure 2: Effect of fabrication parameters on the mean diameter of μCBs, (a) stirring speed (250–1250 rpm), (b) surfactant (Span 80) concentration (0.5–6.0% w/v), (c) cellulose concentration (1–5% w/v), and (d) reaction temperature (30–100°C). Note: other synthesis parameters were being fixed as applicable (3% w/v cellulose solution; 2% w/v Span 80; stirring speed 1000 rpm; 30°C).

3.2. Effect of Stirring Speed. The mean diameter of cellulose beads was observed to be significantly affected by the stirring speed during synthesis (Figure 2(a)). The mean diameter of cellulose beads decreased from the maximum of 64.5±3.9 μm to 29.6 ± 2.0 μm, as the stirring speed was increased from 250 rpm to 1250 rpm. Higher stirring speed provided the higher shearing force needed to reduce the droplet size of microemulsion formed which, in turn, led to decrease in the mean diameter of cellulose beads [35]. The stirring speed of 1000 rpm was found to be the optimum stirring speed for fabricating μCBs with the smallest mean diameter of 27.6 ± 1.0 μm.

3.3. Effect of Surfactant Concentration. The mean diameter of μCBs formed was observed to be significantly affected by the concentration of surfactant presence in the water-in-oil microemulsion (Figure 2(b)). The mean diameter of μCBs decreased linearly from the maximum of about 50 μm to 26 μm as the concentration of surfactant was increased from 0.5 to 3.0% (w/v) but thereafter had remained almost constant at about 30 μm at surfactant concentrations of 4.0 to 6.0% (w/v). Cellulose beads of the smallest mean diameter (26.5 ± 2.1 μm) were obtained at 3% (w/v) Span 80 which corresponded to the critical micelle concentration of Span 80 at 0.2 mM [36]. Above the critical micelle concentration of Span 80, the droplet size of microemulsion would be almost constant and hence the mean diameter of cellulose beads was observed to remain constant at about 30 μm [37]. A surfactant concentration of 3% w/v and above would be optimal for providing complete coverage of the entire surface area of microemulsion droplets in order to afford maximum stability against coalescence and to maintain the smallest emulsion droplet size [38]. In contrast, μCBs of larger mean diameter were obtained at lower surfactant concentration (<3.0% w/v), as microemulsion droplets tend to coalesce with each other to form larger droplets in order to reduce their surface area or energy. Tong et al. [39] reported similar results regarding the effect of surfactant concentration on the mean size of microspheres formed.

3.4. Effect of Cellulose Concentration. μCBs were fabricated from cellulose solution of various concentrations (1–5% w/v) at fixed stirring speed of 1000 rpm and Span 80 concentration of 3.0% w/v (Figure 2(c)). The mean diameter of cellulose beads was observed to increase linearly from 14.5 ± 3.3 μm to 42.3 ± 3.6 μm with increasing cellulose concentrations of

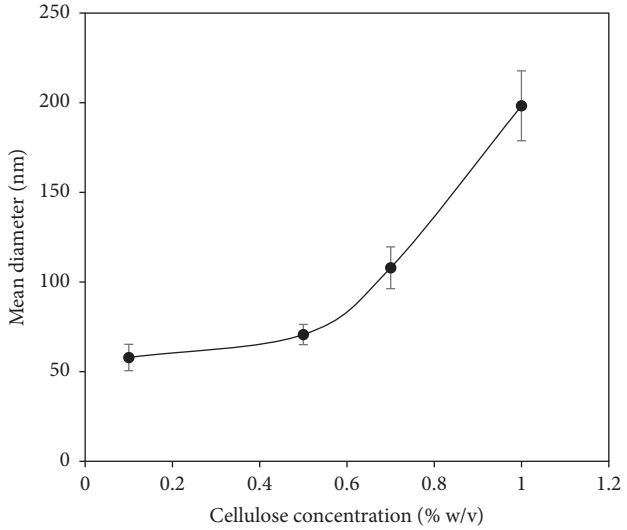

Figure 3: Effect of cellulose solution concentration on the mean diameter of nCBs formed.

1–5% w/v. The increase in the mean diameter of μCBs could be due to increased viscosity at higher cellulose concentrations, which would, in turn, lead to the formation of larger microemulsion droplets, and hence μCBs of larger mean diameters were formed [38].

3.5. Effect of Reaction Temperature. The effect of reaction temperature on the mean diameter of cellulose beads fabricated at temperatures within the range of 30°C to 100°C is shown in Figure 2(d). The mean diameter of cellulose beads was observed to increase nonlinearly with increasing reaction temperature. The mean diameters of cellulose beads formed were 26.1 ± 1.9 μm and 67.2 ± 3.6 μm at reaction temperatures of 30°C and 100°C, respectively. The observed increase in the mean diameter of cellulose beads with increased reaction temperature could be attributed to the instability of microemulsion droplets at higher temperatures which promoted coalescence of microemulsion droplets and hence the formation of cellulose beads with larger mean diameters [40]. Besides, the critical micelle concentration of Span 80 could be affected at higher reaction temperatures leading to the formation of larger microemulsion droplet sizes. In addition, the effectiveness of interfacial adsorption of surfactant could be affected at higher reaction temperatures. The higher kinetic energy could lead to desorption of loosely adsorbed surfactant molecules from microemulsion droplets at the water-oil interface. The destabilization of water-in-oil microemulsion droplets due to increased collision and coalescence rates at higher reaction temperature would eventually lead to increased mean diameter of cellulose beads [41].

3.6. Fabrication of Nanosized Cellulose Beads (nCBs). nCBs were fabricated using the nanoprecipitation process in absolute ethanol. The mean diameter of nCBs was observed to increase nonlinearly with higher concentration of cellulose solution as shown in Figure 3. nCBs of the smallest and largest mean diameter of 57 ± 2.3 nm and 200 ± 2.3 nm were obtained at cellulose solution concentrations of 0.1% w/v and 1.0% w/v, respectively. At low cellulose solution concentration, cellulose molecules would undergo complete nucleation process which resulted in the precipitation of nCBs in a more dispersed state [24, 42]. As the concentration of cellulose solution was increased, the Ostwald ripening effect would lead to the formation of larger cellulose beads which grew at the expense of smaller cellulose beads [25]. Besides, the hydrophilic nature of cellulose molecules would lead to aggregation through hydrogen bonding between smaller cellulose to form larger cellulose beads [43]. The synthesis procedure used in the current study afforded precise control of the mean diameter of cellulose beads within the ranges of 57 ± 2.3 nm to 200 ± 2.3 nm. In contrast, highly agglomerated cellulose nCBs were reported by Kumar and coworkers [44]. Our synthesis procedure had also avoided the usage of highly corrosive sulfuric acid [35].

3.7. Characterization of Cellulose Beads. Both SEM and TEM were used to investigate the morphological characteristics of cellulose beads. Figure 4(a) shows the SEM micrograph of μCBs with mean diameter of 27.7 ± 1.2 μm obtained from 3% w/v cellulose solution. The morphology of nCBs with mean diameter of 70.0 ± 2.8 nm is shown in Figures 4(b) and 4(c). Both μCBs and nCBs were mostly spherical in shape. nCBs showed some degree of aggregation mainly due to strong van der Waals force and electrostatic attraction between cellulose molecules [23, 45]. Most notably, the BET specific surface area of nCBs was substantially higher at 214 m^2/g as compared to that of μCBs at 127 m^2/g (Figure 4(d)), indicating that the overall surface area of cellulose beads would increase substantially with decrease in their mean diameters.

3.8. Loading and Release Kinetics of Curcumin

3.8.1. Loading of Curcumin. The mean diameter of cellulose beads was observed to substantially affect the loading capacity and loading efficiency of curcumin onto cellulose beads. As shown in Table 1 and Figure 5, the highest loading efficiency of curcumin (~95%) was achieved for cellulose beads with the smallest mean diameter range of 40–90 nm. As the mean diameter of cellulose beads increased from nanometer to micrometer ranges (i.e., 100–130 nm, 190–250 nm, 20–40 μm, and 41–60 μm), the loading efficiency of curcumin was observed to decrease substantially from 79% to 65%. Cellulose beads with the largest mean diameter range of 61–80 μm were observed to exhibit the lowest curcumin loading efficiency (57%). Both loading capacity and loading efficiency exhibited a strong inverse linear relationship with the mean diameter range of cellulose beads with R^2 of 0.9576 and 0.9562, respectively. Cellulose beads of larger mean diameter possess considerably lower surface-to-volume ratio as compared to that of cellulose beads of smaller mean diameters. Typically, the drug loading capacity and loading efficiency are dependent on the overall exposed surface area for drug uptake via either diffusional or surface adsorption processes. Henceforth, both the loading capacity and loading efficiency of cellulose beads could be substantially enhanced

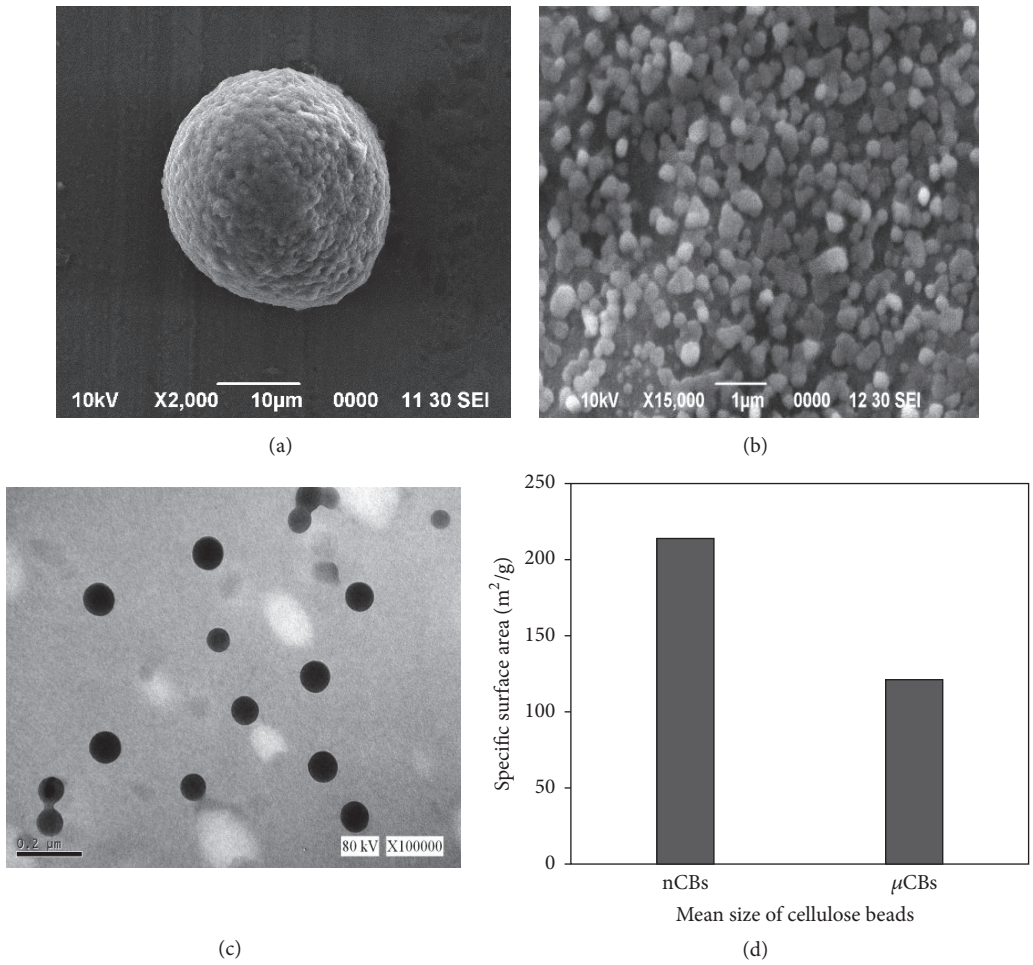

Figure 4: SEM micrographs of cellulose beads, (a) μCBs, and (b) nCBs; (c) TEM micrograph of nCBs, and (d) BET specific surface areas of nCBs and μCBs.

Table 1: Effect of mean diameter range of cellulose beads on loading capacity and efficiency of curcumin.

Mean diameter range	Loading capacity (mg/g)	Loading efficiency (%)
nCBs (nm)		
40–90	1.13 ± 0.03	94.5 ± 2.5
100–130	0.95 ± 0.09	79.4 ± 1.8
190–250	0.91 ± 0.02	76.0 ± 1.7
μCBs (μm)		
20–40	0.83 ± 0.05	69.7 ± 3.9
41–60	0.77 ± 0.03	64.6 ± 1.8
61–80	0.68 ± 0.02	56.9 ± 1.5

Values represent the means ± SD; $n = 3$.

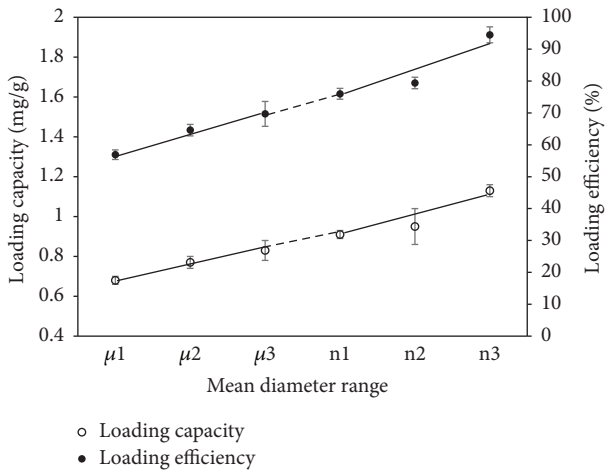

Figure 5: Effect of mean diameter range of cellulose beads on the loading capacity and efficiency of curcumin.

by simply controlling their mean diameter ranges. Francis et al. [46] reported similar findings that the drug loading efficiency increased with decreased in the mean diameter of poly(3-hydroxybutyrate) beads.

3.8.2. Release Kinetics of Curcumin. Figure 6 shows the release kinetic profiles, cumulative percentage release, and

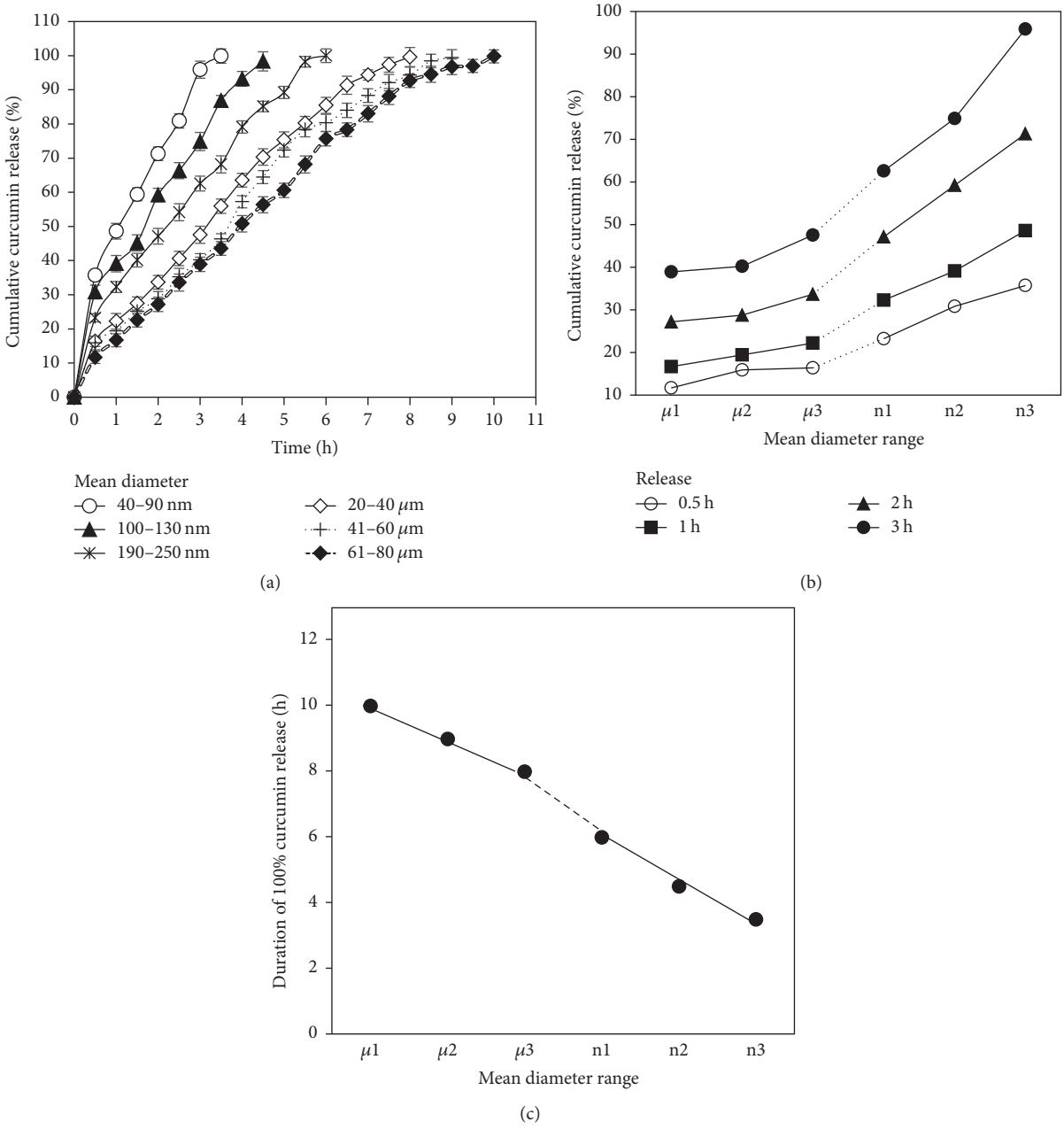

Figure 6: (a) Release kinetic profiles of curcumin from cellulose beads of different mean diameter ranges, (b) cumulative percentage of curcumin released from cellulose beads of various mean diameter ranges at different time intervals, and (c) durations for 100% curcumin released from cellulose beads of different mean diameter ranges (μ1: 61–80 μm, μ2: 41–60 μm, μ3: 20–40 μm, n1: 190–250 nm, n2: 100–130 nm, and n3: 40–90 nm).

the duration of complete (100%) release of curcumin from cellulose beads with different mean diameter ranges. The rates of curcumin release from cellulose beads were observed to be highly dependent on their mean diameter ranges as evidenced by the different slopes of their release kinetic profiles (Figure 6(a)). Cellulose beads of smaller mean diameter were observed to exhibit substantially higher release rate as compared with those of cellulose beads of larger mean diameter.

As shown in Figure 6(b), cellulose beads of the smallest mean diameter range (40–90 nm) exhibited the highest cumulative percentage release of curcumin (35.7%) within initial 0.5 h. In contrast, cellulose beads with the largest mean diameter range (61–80 μm) exhibited the lowest cumulative percentage release of curcumin (11.6%) which was more than three times lower than that of smallest cellulose beads. Generally, the cumulative percentage release of curcumin from cellulose beads at various release durations was inversely proportional to their mean diameter ranges.

Table 2: Release kinetic parameters of curcumin from cellulose beads of different mean diameter ranges.

Mean diameter range	Zero order	Higuchi model	Korsmeyer-Peppas model		
	(R^2)	(R^2)	(R^2)	n	k_{KP} (h^{-n})
nCBs (nm)					
40–90	0.992	0.987	0.990	0.544	1.698
100–130	0.993	0.993	0.973	0.561	1.612
190–250	0.994	0.9851	0.991	0.608	1.516
μCBs (μm)					
20–40	0.986	0.984	0.986	0.717	1.359
41–60	0.984	0.977	0.971	0.730	1.311
61–80	0.983	0.983	0.992	0.782	1.239

The durations for complete (100%) curcumin release (3–10 h) from cellulose beads as a function of their mean diameter range is shown in Figure 6(c). Evidently, the duration for complete curcumin release was observed to be inversely proportional to the mean diameter range of cellulose beads. For nCBs with mean diameter range of 40–90 nm, up to 99.8% of curcumin was being released within 3 h whereas μCBs with mean diameter range of 61–80 μm exhibited sustained release duration of about 10 h. These observations could be attributed to higher surface area-to-volume ratios of cellulose beads with smaller mean diameter [47]. The surface area-to-volume ratio of nCBs is more than 40% higher than that of μCBs. Higher surface area-to-volume ratio would lead to higher exposure to the releasing medium (PBS) and hence the enhanced rate of curcumin release [48].

In order to elucidate the release mechanisms of curcumin from cellulose beads dispersed in PBS in the presence of SDS, different kinetic models were fitted and the release kinetic parameters are presented in Table 2. The linear regression coefficients (R^2) of zero-order kinetic for cellulose beads of various diameter ranges were within the range of 0.983–0.994 indicating that the release of curcumin from cellulose beads was independent of its concentration. Various mass transfer phenomena such as water and curcumin diffusion as well as physical characteristics such as surface area-to-volume ratio and swelling of cellulose beads could have contributed to the overall zero-order kinetics of curcumin release. Besides, the release of curcumin from cellulose beads of different mean diameter ranges exhibited very good fit to the Higuchi's kinetic model ($R^2 > 0.97$) indicating that the release of curcumin from cellulose beads could be attributed to diffusional processes. To further elucidate the release mechanism of curcumin, in vitro release data were being fitted to the Korsmeyer-Peppas empirical kinetic model. Cellulose beads of various mean diameter ranges showed very good fit (R^2 = 0.97–0.99) with the slope (n) values within the range of 0.43–0.85 indicating that the release mechanism of curcumin from cellulose beads was anomalous or non-Fickian diffusion release processes [49]. As such, the mean diameter ranges of CBs exhibited dominant effects on the release kinetic profiles of curcumin, which could be precisely controlled by simply tailoring the mean diameter ranges of CBs.

4. Conclusion

Spherical cellulose beads of controllable sizes from micrometer to nanometer mean diameter ranges were successfully fabricated from cellulose fibres of paper wastes under controlled conditions. The mean diameter of cellulose beads was shown to be the primary determinant of loading capacity and loading efficiency, as well as the release kinetic profiles of curcumin. Both μCBs and nCBs exhibited similar release kinetic profiles of curcumin which conformed well to the zero-order kinetics and the Higuchi kinetics model. The release mechanism of curcumin from cellulose beads was mainly attributed to diffusional processes. Henceforth, further optimization of the delivery characteristics of curcumin via precisely tailoring the mean diameter ranges of cellulose beads is therefore highly envisaged.

Conflicts of Interest

The authors do not have any conflicts of interest.

Acknowledgments

The authors wish to acknowledge the financial support rendered by the Malaysian Ministry of Higher Education (MOHE) via the award of fundamental research grants (Grant nos. FRGS/ST01(01)/967/2013(08) and F07/FRGS/1495/2016), as well as research management and support provided by the Research Innovation and Management Centre (RIMC), Universiti Malaysia Sarawak.

References

[1] H. Zhu, W. Luo, P. N. Ciesielski et al., "Wood-Derived Materials for Green Electronics, Biological Devices, and Energy Applications," *Chemical Reviews*, vol. 116, no. 16, pp. 9305–9374, 2016.

[2] S.-F. Chin, F. B. Jimmy, and S.-C. Pang, "Fabrication of cellulose aerogel from sugarcane bagasse as drug delivery carriers," *Journal of Physical Science*, vol. 27, no. 3, pp. 159–168, 2016.

[3] M. F. Rosa, E. S. Medeiros, J. A. Malmonge et al., "Cellulose nanowhiskers from coconut husk fibers: effect of preparation conditions on their thermal and morphological behavior," *Carbohydrate Polymers*, vol. 81, no. 1, pp. 83–92, 2010.

[4] H. Sehaqui, M. Allais, Q. Zhou, and L. A. Berglund, "Wood cellulose biocomposites with fibrous structures at micro- and nanoscale," *Composites Science and Technology*, vol. 71, no. 3, pp. 382–387, 2011.

[5] J. Shokri and K. Adibkia, "Application of cellulose and cellulose derivatives in pharmaceutical industries," *Cellulose-Medical, Pharmaceutical and. Electronic Applications*, vol. 1, pp. 1–65, 2013.

[6] R. Girija Aswathy, B. Sivakumar, D. Brahatheeswaran et al., "Multifunctional Biocompatible Fluorescent Carboxymethyl Cellulose Nanoparticles," *Journal of Biomaterials and Nanobiotechnology*, vol. 3, no. 2, pp. 254–261, 2012.

[7] I. I. Muhamad, L. S. Fen, N. H. Hui, and N. A. Mustapha, "Genipin-cross-linked kappa-carrageenan/carboxymethyl cellulose beads and effects on beta-carotene release," *Carbohydrate Polymers*, vol. 83, no. 3, pp. 1207–1212, 2011.

[8] A. Mandal and D. Chakrabarty, "Isolation of nanocellulose from waste sugarcane bagasse (SCB) and its characterization," *Carbohydrate Polymers*, vol. 86, no. 3, pp. 1291–1299, 2011.

[9] H. M. C. Azeredo, L. H. C. Mattoso, D. Wood, T. G. Williams, R. J. Avena-Bustillos, and T. H. McHugh, "Nanocomposite edible films from mango puree reinforced with cellulose nanofibers," *Journal of Food Science*, vol. 74, no. 5, pp. N31–N35, 2009.

[10] A. Kaushik, M. Singh, and G. Verma, "Green nanocomposites based on thermoplastic starch and steam exploded cellulose nanofibrils from wheat straw," *Carbohydrate Polymers*, vol. 82, no. 2, pp. 337–345, 2010.

[11] X. Luo, J. Zeng, S. Liu, and L. Zhang, "An effective and recyclable adsorbent for the removal of heavy metal ions from aqueous system: Magnetic chitosan/cellulose microspheres," *Bioresource technology*, vol. 194, pp. 403–406, 2015.

[12] X. Sun, L. Yang, Q. Li et al., "Amino-functionalized magnetic cellulose nanocomposite as adsorbent for removal of Cr(VI): Synthesis and adsorption studies," *Chemical Engineering Journal*, vol. 241, pp. 175–183, 2014.

[13] B. Patel, V. Modi, K. Patel, and M. Patel, "Preparation and evaluation of ethyl cellulose microspheres prepared by emulsification-solvent evaporation method," *International Journal Research in Management and Pharmacy*, vol. 1, no. 1, pp. 82–91, 2012.

[14] M. Li, O. Rouaud, and D. Poncelet, "Microencapsulation by solvent evaporation: state of the art for process engineering approaches," *International Journal of Pharmaceutics*, vol. 363, no. 1-2, pp. 26–39, 2008.

[15] B. Nath, L. K. Nath, B. Mazumder, P. Kumar, N. Sharma, and B. P. Sahu, "Preparation and characterization of salbutamol sulphate loaded ethyl cellulose microspheres using water-in-oil-oil emulsion technique," *Iranian Journal of Pharmaceutical Research*, vol. 9, no. 2, pp. 97–105, 2010.

[16] N. Chella, K. K. Yada, and R. Vempati, "Preparation and evaluation of ethyl cellulose microspheres containing diclofenac Sodium by novel W/O/O emulsion method," *Journal of Pharmaceutical Sciences and Research*, vol. 2, no. 12, pp. 884–888, 2010.

[17] B. N. Vedha Hari, A. Brahma Reddy, and B. Samyuktha Rani, "Floating drug delivery of nevirapine as a gastroretentive system," *Journal of Young Pharmacists*, vol. 2, no. 4, pp. 350–355, 2010.

[18] M. A. Malik, M. Y. Wani, and M. A. Hashim, "Microemulsion method: a novel route to synthesize organic and inorganic nanomaterials: 1st Nano Update," *Arabian Journal of Chemistry*, vol. 5, no. 4, pp. 397–417, 2012.

[19] R. P Wankhade, A. R. Pundir, and S. S. Bhalerao, "Microemulsion as novel cosmeceutical drug delivery system," *Journal of Pharmaceutics and Cosmetology*, vol. 2, no. 9, pp. 78–92, 2012.

[20] S. Paul and A. K. Panda, "Physico-chemical studies on microemulsion: Effect of cosurfactant chain length on the phase behavior, formation dynamics, structural parameters and viscosity of water/(Polysorbate-20 + n-Alkanol)/n-heptane water-in-oil microemulsion," *Journal of Surfactants and Detergents*, vol. 14, no. 4, pp. 473–486, 2011.

[21] N. Grampurohit, P. Ravikumar, and R. Mallya, "Microemulsions for topical use- A review," *Indian Journal of Pharmaceutical Education and Research*, vol. 45, no. 1, pp. 100–107, 2011.

[22] J. P. Rao and K. E. Geckeler, "Polymer nanoparticles: preparation techniques and size-control parameters," *Progress in Polymer Science*, vol. 36, no. 7, pp. 887–913, 2011.

[23] A.-M. Shi, D. Li, L.-J. Wang, B.-Z. Li, and B. Adhikari, "Preparation of starch-based nanoparticles through high-pressure homogenization and miniemulsion cross-linking: Influence of various process parameters on particle size and stability," *Carbohydrate Polymers*, vol. 83, no. 4, pp. 1604–1610, 2011.

[24] Y. Tan, K. Xu, L. Li, C. Liu, C. Song, and P. Wang, "Fabrication of size-controlled starch-based nanospheres by nanoprecipitation," *ACS Applied Materials and Interfaces*, vol. 1, no. 4, pp. 956–959, 2009.

[25] S. F. Chin, S. C. Pang, and S. H. Tay, "Size controlled synthesis of starch nanoparticles by a simple nanoprecipitation method," *Carbohydrate Polymers*, vol. 86, no. 4, pp. 1817–1819, 2011.

[26] H. Wang, D. Li, and R. Zhang, "Preparation of ultralong cellulose nanofibers and optically transparent nanopapers derived from waste corrugated paper pulp," *BioResources*, vol. 8, no. 1, pp. 1374–1384, 2013.

[27] H. Jin, C. Zha, and L. Gu, "Direct dissolution of cellulose in NaOH/thiourea/urea aqueous solution," *Carbohydrate Research*, vol. 342, no. 6, pp. 851–858, 2007.

[28] K. I. Priyadarsini, "The chemistry of curcumin: from extraction to therapeutic agent," *Molecules*, vol. 19, no. 12, pp. 20091–20112, 2014.

[29] Z. Minpeng and L. Suhong, "The stability of curcumin and drug-loading property of starch microspheres for it," *Advanced in Biomedical Engineering*, vol. 9, no. 1, 44 pages, 2012.

[30] P. Costa and J. M. Sousa Lobo, "Modeling and comparison of dissolution profiles," *European Journal of Pharmaceutical Sciences*, vol. 13, no. 2, pp. 123–133, 2001.

[31] S. Dash, P. N. Murthy, L. Nath, and P. Chowdhury, "Kinetic modeling on drug release from controlled drug delivery systems," *Acta Poloniae Pharmaceutica—Drug Research*, vol. 67, no. 3, pp. 217–223, 2010.

[32] X. Luo, S. Liu, J. Zhou, and L. Zhang, "In situ synthesis of Fe_3O_4/cellulose microspheres with magnetic-induced protein delivery," *Journal of Materials Chemistry*, vol. 19, no. 21, pp. 3538–3545, 2009.

[33] M. Madhavi, K. Madhavi, and A. V. Jithan, "Preparation and in vitro/in vivo characterization of curcumin microspheres intended to treat colon cancer," *Journal of Pharmacy and Bioallied Sciences*, vol. 4, no. 2, pp. 164–171, 2012.

[34] M. K. Nkansah, D. Thakral, and E. M. Shapiro, "Magnetic poly(lactide-co-glycolide) and cellulose particles for MRI-based cell tracking," *Magnetic Resonance in Medicine*, vol. 65, no. 6, pp. 1776–1785, 2011.

[35] B. S. Purkait, D. Ray, S. Sengupta, T. Kar, A. Mohanty, and M. Misra, "Isolation of cellulose nanoparticles from sesame husk,"

Industrial and Engineering Chemistry Research, vol. 50, no. 2, pp. 871–876, 2011.

[36] H. Zhou, Y. Yao, Q. Chen, G. Li, and S. Yao, "A facile microfluidic strategy for measuring interfacial tension," *Applied Physics Letters*, vol. 103, no. 23, Article ID 234102, 2013.

[37] E. L. Michor and J. C. Berg, "Temperature Effects on Micelle Formation and Particle Charging with Span Surfactants in Apolar Media," *Langmuir*, vol. 31, no. 35, pp. 9602–9607, 2015.

[38] S. F. Chin, A. Azman, and S. C. Pang, "Size controlled synthesis of starch nanoparticles by a microemulsion method," *Journal of Nanomaterials*, vol. 2014, Article ID 763736, 2014.

[39] J. Tong, M. Nakajima, H. Nabetani, and Y. Kikuchi, "Surfactant effect on production of monodispersed microspheres by microchannel emulsification method," *Journal of Surfactants and Detergents*, vol. 3, no. 3, pp. 285–293, 2000.

[40] K. Shinoda and H. Saito, "The Stability of O/W type emulsions as functions of temperature and the HLB of emulsifiers: The emulsification by PIT-method," *Journal of Colloid And Interface Science*, vol. 30, no. 2, pp. 258–263, 1969.

[41] G. Chen and D. Tao, "An experimental study of stability of oil-water emulsion," *Fuel Processing Technology*, vol. 86, no. 5, pp. 499–508, 2005.

[42] S. Hornig, T. Heinze, C. R. Becer, and U. S. Schubert, "Synthetic polymeric nanoparticles by nanoprecipitation," *Journal of Materials Chemistry*, vol. 19, no. 23, pp. 3838–3840, 2009.

[43] C. Bilbao-Sáinz, R. J. Avena-Bustillos, D. F. Wood, T. G. Williams, and T. H. Mchugh, "Composite edible films based on hydroxypropyl methylcellulose reinforced with microcrystalline cellulose nanoparticles," *Journal of Agricultural and Food Chemistry*, vol. 58, no. 6, pp. 3753–3760, 2010.

[44] S. Kumar, Y. S. Negi, and J. S. Upadhyaya, "Studies on characterization of corn cob based nanoparticles," *Advanced Materials Letters*, vol. 1, no. 3, pp. 246–253, 2010.

[45] J. Liu, F.-H. Wang, L.-L. Wang et al., "Preparation of fluorescence starch-nanoparticle and its application as plant transgenic vehicle," *Journal of Central South University of Technology (English Edition)*, vol. 15, no. 6, pp. 768–773, 2008.

[46] L. Francis, D. Meng, J. Knowles, T. Keshavarz, A. R. Boccaccini, and I. Roy, "Controlled delivery of gentamicin using poly(3-hydroxybutyrate) microspheres," *International Journal of Molecular Sciences*, vol. 12, no. 7, pp. 4294–4314, 2011.

[47] H. K. Makadia and S. J. Siegel, "Poly Lactic-*co*-Glycolic Acid (PLGA) as biodegradable controlled drug delivery carrier," *Polymers*, vol. 3, no. 3, pp. 1377–1397, 2011.

[48] F. Sadeghi, F. Mosaffa, and H. A. Garekani, "Effect of particle size, compaction force and presence of aerosil 200 on the properties of matrices prepared from physical 70 mixture of propranolol hydrochloride and eudragit RS or RL," *Iranian Journal of Basic Medical. Sciences*, vol. 10, no. 3, pp. 197–205, 2007.

[49] J. Siepmann and F. Siepmann, "Mathematical modeling of drug delivery," *International Journal of Pharmaceutics*, vol. 364, no. 2, pp. 328–343, 2008.